Frequency-Variation Sensors for Permittivity Measurements Based on Dumbbell-Shaped Defect Ground Structures (DB-DGS): Analytical Method and Sensitivity Analysis

Jonathan Muñoz-Enano, *Student Member, IEEE*, Paris Vélez, *Senior Member, IEEE*, Marta Gil, *Member, IEEE*, and Ferran Martín, *Fellow, IEEE*

***Abstract*—It is shown in this paper that a microstrip line loaded with a dumbbell-shaped defect ground structure (DB-DGS) is useful for complex permittivity measurements. The working principle of the sensor is the variation in the notch (resonance) frequency and depth caused by the material under test (MUT), when it is put in contact with the sensitive region of the device, i.e., the capacitive slot. It is demonstrated that the relative sensitivity of the sensor, defined as the variation of the resonance frequency of the DB-DGS with the dielectric constant of the MUT relative to the resonance frequency of the bare structure, does not depend on the geometry of the DB-DGS, provided the substrate is thick enough. The relative sensitivity, the key figure of merit, is dictated by the equivalent dielectric constant of the substrate, and it increases as the substrate permittivity decreases. Using the circuit model of the sensing structure, simple analytical expressions providing the dielectric constant and the loss tangent of the MUT are derived. Such analytical formulas depend on the notch frequency and depth of the sensor with and without MUT in contact with it, i.e., easily measurable quantities. The analysis carried out is corroborated through full-wave electromagnetic simulation and experiments.**

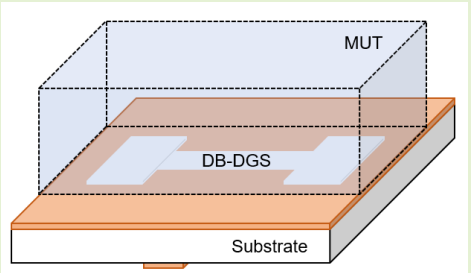

***Index Terms*— Microwave sensors, permittivity sensors, defect ground structures (DGS), microstrip technology.**

I. Introduction

Planar resonant elements have been exhaustively used for sensing purposes using microwaves. The main reasons are the high sensitivity, low cost, small size, and the inherent integration potential of planar microwave resonators. This latter aspect is fundamental in order to implement low-profile planar sensors, such as many applications demand, including sensors combined with microfluidic technology, of interest for liquid characterization and bio-sensing [1]-[15].

Most microwave resonant sensors are implemented by loading a transmission line with a planar resonator (the sensing element), and the most usual working principle is frequency variation [2],[4],[6],[10],[16]-[20]. Nevertheless, sensors based on symmetry truncation, including frequency-splitting sensors [8],[21]-[25], coupling-modulation sensors [26]-[35], and differential sensors [9],[13]-[15],[36] have also been reported. As compared to those sensors that exploit frequency variation, sensors based on symmetry disruption are typically more robust against cross-sensitivities related to ambient factors (temperature, humidity, etc.) [37]. Moreover, calibration in symmetry-based sensors is not always required, as far as a reference material with well-known properties is typically used for sensing. Highly-sensitive differential sensors, e.g., devices able to detect extremely small concentrations of solutes in diluted solutions, have been reported [9],[13],[15]. Despite these relevant advantageous aspects of symmetry-based sensors, frequency-variation sensors are still highly demanded since they are inherently simpler, cheaper and smaller, provided a single resonant element suffices for sensing purposes. Nevertheless, it should be mentioned that phase-variation sensors, operating in reflection, based on a planar resonant element (either semi-lumped or distributed), have been recently reported and demonstrated to exhibit very competitive performance [38],[39].

Several types of planar resonant elements have been used for the implementation of frequency-variation sensors, including split ring resonators (SRRs) [2], complementary split ring resonators (CSRRs) [4],[6],[10],[18],[19], step impedance

This work was supported by MINECO-Spain (project PID2019-103904RB-I00), Generalitat de Catalunya (project 2017SGR-1159), Institució Catalana de Recerca i Estudis Avançats (who awarded Ferran Martín), and by FEDER funds. J. Muñoz-Enano acknowledges Secreteraria d'Universitats i Recerca (Gen. Cat.) and European Social Fund for the FI grant.

J. Muñoz-Enano, P. Vélez, and F. Martín are with GEMMA/CIMITEC, Departament d'Enginyeria Electrònica, Universitat Autònoma de Barcelona, 08193 Bellaterra, Spain (e-mail: Ferran.Martin@uab.es).

M. Gil is with Audiovisual Engineering and Communications Department, Universidad Politécnica de Madrid, 28031, Madrid, Spain.

shunt stubs [40], and other related resonant elements. In this paper, a frequency-variation sensor useful for complex permittivity measurements, based on a microstrip line loaded with a dumbbell-shaped defect ground structure (DB-DGS), is presented. The DB-DGS [41] element is a slot resonator, transversally etched in the ground plane of the microstrip line, with a resonance frequency very sensitive to the permittivity of the surrounding material. The purpose of the paper is twofold. A first objective is to demonstrate that the relative sensitivity, a figure of merit in frequency-variation sensors, only depends on the so-called equivalent dielectric constant of the substrate, to be defined later. The second objective is to obtain analytical expressions useful to determine the material parameters of the material under test (MUT), i.e. the dielectric constant and the loss tangent, from the measurement of the transmission coefficient of the sensor, the DB-DGS-loaded line. The results of the analysis will be validated from full-wave electromagnetic simulations and through the measurement of the complex dielectric constant of several materials, including solid samples and deionized (DI) water. It should be mentioned that in [42], a differential-mode sensor based on a pair of DB-DGS-loaded lines was reported. Nevertheless, in that sensor the output variable was the magnitude of the cross-mode transmission coefficient.

The work is organized as follows: Section II presents the proposed sensor and the lumped element equivalent circuit, necessary for the analysis. The validity of the model is demonstrated in this section, by comparing electromagnetic simulations of the response of the designed structure with circuit simulations with extracted parameters. Section III presents the sensitivity analysis, validated by considering several case examples. The analytical expressions providing the dielectric constant and loss tangent of the MUT are derived in Section IV. The validity of these expressions is demonstrated at simulation level and experimentally, by considering different structures (with different dielectric constant and loss factor), in Section V. A comparative analysis is carried out in Section VI. Finally, Section VII highlights the main conclusions.

II. Proposed DB-DGS based sensor and circuit model

The typical topology of the proposed sensor and the circuit model are depicted in Fig. 1 (the justification of such model is reported in a recent paper by some of the authors [43]). The sensor consists of a microstrip line with a DB-DGS resonator transversally etched in the ground plane. The DB-DGS is modeled by the resonant tank formed by the capacitance C (the slot capacitance) and by the inductance L (related to the return current path in the ground plane and dictated by the perimeter of the resonator). The conductance G accounts for substrate losses, i.e., it is assumed that metallic losses have negligible effect. The presence of a dielectric material (MUT) in contact with the DB-DGS is taken into account by including two additional elements, C_{MUT} and G_{MUT}. The former accounts for the enhancement of the DB-DGS capacitance due to the presence of the MUT, and it is related to the dielectric constant of the MUT, ε_{MUT}. The conductance G_{MUT} is introduced in order to include the effects of losses in the MUT, and it is related to its loss tangent. Obviously, in the bare sensor, C_{MUT} and G_{MUT} are null. Finally, βl and Z_0 are the electrical length and characteristic impedance, respectively, of the microstrip line, β and l being the phase constant and the physical length, respectively, of the line.

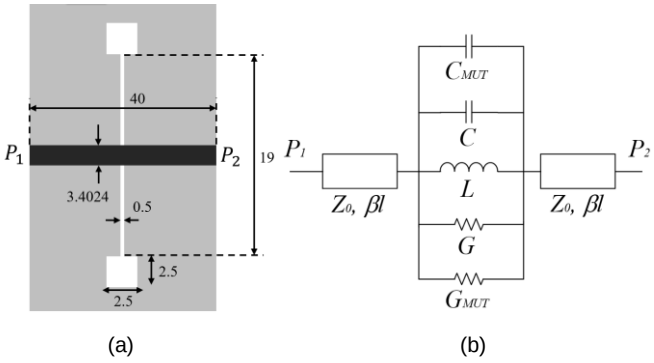

Fig. 1. Typical topology (a) and circuit model (b) of the proposed DB-DGS-based permittivity sensor. Dimensions are given in mm. Ground plane in grey.

The model has been validated by first extracting the circuit parameters in the structure without the presence of MUT. For that purpose, we have considered the dimensions indicated in the caption of Fig. 1, and the parameters of the *Rogers 4003C* substrate with dielectric constant ε_r = 3.55, thickness h = 1.524 mm and loss factor tanδ = 0.0022. With these substrate parameters, the electrical length of the line and the characteristic impedance are βl = 147º (at the notch frequency f_0) and Z_0 = 50 Ω, respectively. The parameters describing the bare DB-DGS have been extracted from the full-wave electromagnetic simulation response (depicted in Fig. 2 and obtained by means of *ANSYS HFSS*). For that purpose, the resonance frequency, f_0, and the susceptance slope at f_0 have been used. This provides the reactive elements L and C, whereas G has been determined by curve fitting the response (it is dictated by the notch magnitude). The extracted parameters are indicated in Table I. Using these parameters, we have obtained the circuit response of the structure (using *Keysight ADS*), also depicted in Fig. 2. The agreement is very good, pointing out the validity of the model.

Nevertheless, we have also obtained the electromagnetically simulated response by considering the DB-DGS loaded with a semi-infinite MUT, with dielectric constant and loss factor ε_{MUT} = 4.4 and tanδ$_{MUT}$ = 0.02, respectively. The results are also depicted in Fig. 2. We have then extracted the parameters by leaving L unaltered, since this parameter is not affected by the presence of the MUT. The values of C_{MUT} and G_{MUT} that are necessary to fit the electromagnetic simulation are indicated in Table I (note that C_{MUT} and G_{MUT} have been actually obtained by subtracting C and G, respectively to the extracted parameters). The circuit response obtained with these parameters is compared to the electromagnetic response in Fig. 2, and, again, good agreement is obtained. According to these results, it is clear that the presence of the MUT can be taken into account by including C_{MUT} and G_{MUT} in the circuit model.

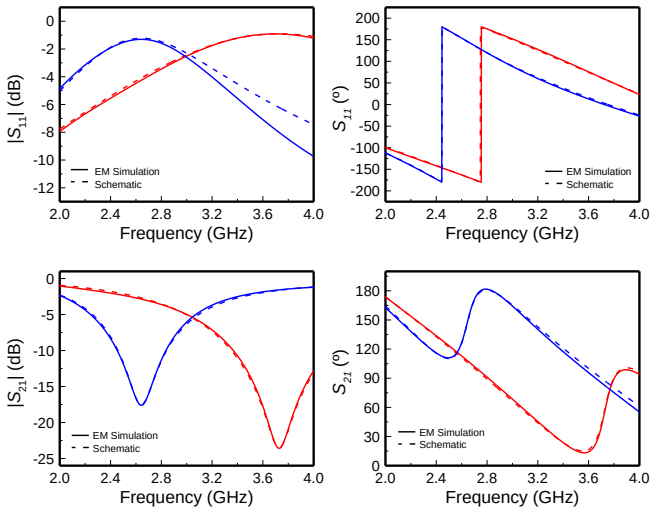

Fig. 2. Response of the considered DB-DGS based sensor without (red curve) and with (blue curve) MUT.

TABLE I
PARAMETER EXTRACTION

	L (nH)	*C* (pF)	*G* (mS)	C_{MUT} (pF)	G_{MUT} (mS)
Bare	2.50	0.73	0.71	----	----
With MUT	2.50	0.73	0.71	0.74	0.40

III. SENSITIVITY ANALYSIS

In frequency-variation permittivity sensors, a figure of merit is the so-called relative sensitivity, defined as follows:

$$\bar{S} = \frac{1}{f_0}\frac{df_0}{d\varepsilon_{MUT}} \tag{1}$$

where the output variable, f_0, is the frequency of the resonant element (the notch frequency in the considered DB-DGS structure), and the input variable is the dielectric constant of the MUT, ε_{MUT}. Normalization to f_0 is due to the fact that working at high frequencies intrinsically provides higher excursion of the resonance frequency (for a given variation of the dielectric constant of the MUT sample). Thus, for comparison purposes, the relative sensitivity, as defined in (1), is the key (representative) sensor parameter. The resonance frequency is given by

$$f_o = \frac{1}{2\pi\sqrt{LC'_{MUT}}} \tag{2}$$

where

$$C'_{MUT} = C + C_{MUT} = C\,\frac{\varepsilon_{r,eq} + \varepsilon_{MUT}}{\varepsilon_{r,eq} + 1} \tag{3}$$

where $\varepsilon_{r,eq}$ is the equivalent dielectric constant of the substrate. Such dielectric constant is defined as the dielectric constant of a hypothetical semi-infinite substrate providing the same contribution to the capacitance of the DB-DGS resonator [44]. Thus, the equivalent dielectric constant coincides with the dielectric constant of the substrate ($\varepsilon_{r,eq} = \varepsilon_r$), provided the substrate is thick enough, so that it can be considered to be semi-infinite in the vertical direction (i.e., with the field lines generated in the slot resonator not reaching the opposite interface). If the semi-infinite substrate approximation is not applicable, the most usual case, then $\varepsilon_{r,eq}$ in (3) must be used, and $\varepsilon_{r,eq} < \varepsilon_r$. Concerning the MUT, it should be semi-infinite in the vertical direction for the validity of expression (3) [10]. In practice, it suffices to consider a finite MUT sample extending beyond the region occupied by the DB-DGS perimeter, with thickness enough to consider that the electric field lines generated by the DB-DGS do not reach the MUT/air interface.

Introducing (2) in (1) gives

$$\bar{S} = -\frac{1}{2(\varepsilon_{r,eq} + \varepsilon_{MUT})} \tag{4}$$

and from this simple expression, it follows that the relative sensitivity does not explicitly depend on the geometry of the DB-DGS resonator (and line). Indeed, for thick enough (semi-infinite) substrates, the relative sensitivity does neither depend on the thickness of the substrate (since $\varepsilon_{r,eq} = \varepsilon_r$ in this case). Since the dielectric constant of the MUT is not a design parameter, the main conclusion of this simple analysis is that the relative sensitivity in DB-DGS-based microstrip permittivity sensors increases as the dielectric constant of the substrate decreases (this is true regardless of the thickness of the substrate). However, for high dielectric constant MUTs, e.g., liquids, the relative sensitivity is dominated by the value of such dielectric constant (since $\varepsilon_{MUT} >> \varepsilon_{r,eq}$ for typical substrate materials, with dielectric constants not exceeding a dozen).

In order to validate the previous conclusion in regard to the relative sensitivity, we have considered the sensor of Fig. 1 (sensor A), with $\varepsilon_r = 3.55$, $h = 1.524$ mm and $\tan\delta = 0.0022$, and we have obtained the relative sensitivity by introducing in (1) the resonance frequencies inferred from electromagnetic simulation, as the dielectric constant of the MUT increases. The input dynamic range is comprised between $\varepsilon_{MUT} = 1$, the value corresponding to air (bare DB-DGS), and $\varepsilon_{MUT} = 10.2$. The results are depicted in Fig. 3, where the curve corresponding to the analytical expression (4) is also included for comparison purposes. As it can be appreciated, very good agreement between the theoretical curve and the data points inferred from the simulated values is obtained. As indicated in the figure, the equivalent dielectric constant of the substrate has been found to be $\varepsilon_{r,eq} = 2.15$. Such value has been inferred by considering the response of the bare sensor and the response of the sensor loaded with any MUT with known dielectric constant. Note that the ratio of the squared resonance frequencies is inversely proportional to the ratio of capacitances, and, using (3), $\varepsilon_{r,eq}$ can be easily isolated [44].

Nevertheless, we have considered three additional sensing structures. In one of them (sensor B), the bare DB-DGS resonates at roughly the same frequency, but the geometry is different. In the other one (sensor C), the resonance frequency of the DB-DGS is higher. In sensors B and C, the substrate is identical to the one of sensor A. By contrast, in the last sensing device (sensor D), a thicker substrate is considered (i.e., $h = 2$ mm), whereas the geometry of the DB-DGS is identical to the one of sensor A. The corresponding layouts of the DB-DGSs

for sensors B and C are depicted in Fig. 4, where the dimensions are indicated. The relative sensitivities for these three additional sensing structures, inferred from (1), are also included in Fig. 3. As it can be appreciated, the resulting data points for sensors B, C and D are very similar, and very similar to those of sensor A. The reason is that the equivalent dielectric constants are similar for the four sensors (the theoretical relative sensitivities, as given by 4, are not included in Fig. 3 for sensors B, C and D, but the values of the equivalent dielectric constant are indicated in the caption). Note that in sensors A and C, the equivalent dielectric constant is roughly the same because in these sensors, the ratio between the slot width (s = 0.5 mm) and substrate thickness (h = 1.524 mm) is identical, and the equivalent dielectric constant is determined by the ratio s/h, as discussed in [44].

With this study, based on full-wave electromagnetic simulation, the reported sensitivity analysis, pointing out that the geometry of the DB-DGS and substrate thickness do not significantly affect the relative sensitivity, provided $s/h << 1$, is validated. By contrast, in sensors similar to the one considered in this paper, but based on complementary split ring resonators (CSRRs) [10], the relative sensitivity depends on the geometry of the resonant element and substrate thickness. Moreover, in CSRR-based sensors, the resonance frequency depends on the coupling capacitance between the line and the CSRR, a parameter not affected by the MUT. Consequently, the relative sensitivity in CSRR-based microstrip sensors is not as good as the one achievable with DB-DGSs.

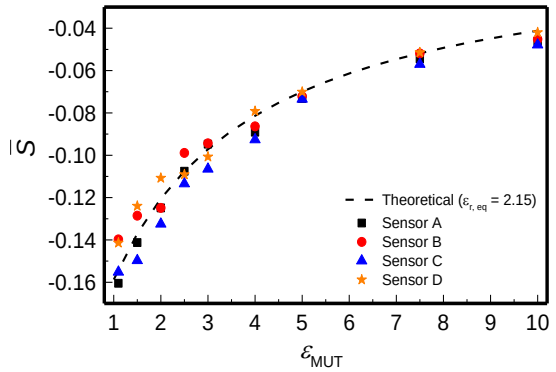

Fig. 3. Dependence of the relative sensitivity with ε_{MUT} for different sensing structures. The dielectric constant of the substrate is ε_r = 3.55 in all cases. The equivalent dielectric constant ($\varepsilon_{r,eq}$) for the Sensor A, B, C and D is 2.15, 2.48, 2.08 and 2.71, respectively.

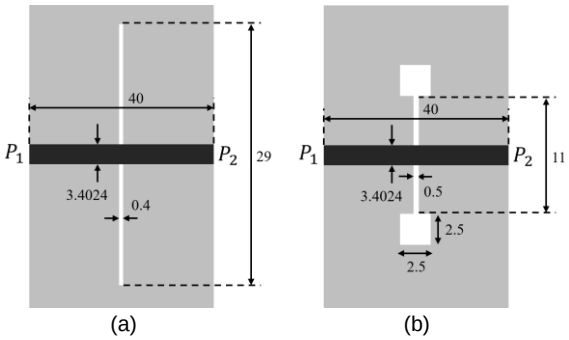

Fig. 4. Layouts of the DB-DGS for sensors B (a) and C (b). Dimensions are given in mm. Ground plane in grey.

IV. Determination of the Dielectric Constant and Loss Tangent of the MUT

In this section, two analytical expressions that provide the dielectric constant, ε_{MUT}, and the loss tangent, $\tan\delta_{MUT}$, of the MUT, from the notch frequency and magnitude of the measured sensor response, are inferred. The hypothesis for the validity of the following analysis is that the thickness of the MUT is enough to avoid the presence of electric field lines in the MUT/air interface (similar to the hypothesis adopted in Section III).

A. Determination of the dielectric constant

The dielectric constant of the MUT can be inferred from the resonance frequencies of the bare sensor, $f_{0,b}$, and sensor loaded with the MUT, $f_{0,MUT}$. Such resonance frequencies are given by (2), with $f_{0,b} = (1/2\pi)(LC)^{-1/2}$, as it is inferred from (2) if ε_{MUT} = 1 (bare DB-DGS). Therefore, these frequencies are related by

$$\frac{f_{0,b}^2}{f_{0,MUT}^2} = \frac{\varepsilon_{r,eq} + \varepsilon_{MUT}}{\varepsilon_{r,eq} + 1} \tag{5}$$

From the previous expression, the dielectric constant of the MUT is found to be

$$\varepsilon_{MUT} = (\varepsilon_{r,eq} + 1)\frac{f_{0,b}^2}{f_{0,MUT}^2} - \varepsilon_{r,eq} \tag{6}$$

Hence, from the knowledge of the equivalent dielectric constant of the substrate, and the measured notch frequencies of the unloaded and loaded sensor, the dielectric constant of the MUT can be obtained.

B. Determination of the loss tangent

The notch magnitude is related to the level of losses of the whole device, including the MUT. Thus, it is expected that the loss tangent of the MUT can be inferred from the measured notch level. If the characteristic impedance of the transmission line sections is Z_0 = 50 Ω, the lines introduce a phase shift in the transmission coefficient, but do not have any influence on its magnitude, given by

$$|S_{21}| = \left| \frac{1}{1 + \frac{1}{2Z_0 Y_{MUT}}} \right| \tag{7}$$

where Y_{MUT} is the admittance of the DB-DGS loaded with the MUT sample, i.e.,

$$Y_{MUT} = G'_{MUT} + j\omega C'_{MUT}\left(1 - \frac{\omega_{0,MUT}^2}{\omega^2}\right) \tag{8}$$

where $G'_{MUT} = G + G_{MUT}$, $\omega = 2\pi f$ is the angular frequency, and $\omega_{0,MUT} = 2\pi f_{0,MUT}$. Expression (8) is also valid for the bare sensor, with $G_{MUT} = 0$ (i.e., $G'_{MUT} = G$), $C_{MUT} = 0$ (that is, $C'_{MUT} = C$), and $\omega_{0,MUT}$ replaced with $\omega_{0,b}$, the resonance (angular) frequency of the bare structure.

For the sensor loaded with the MUT sample, the notch magnitude is given by the transmission coefficient evaluated at $\omega = \omega_{0,MUT}$, that is

$$|S_{21}|_{\omega_{0,MUT}} = \frac{2Z_0 G'_{MUT}}{2Z_0 G'_{MUT} + 1} \quad (9a)$$

Similarly, the notch magnitude for the bare sensor is

$$|S_{21}|_{\omega_{0,b}} = \frac{2Z_0 G}{2Z_0 G + 1} \quad (9b)$$

and combining (9a) and (9b), the conductance contribution of the MUT is found to be

$$G_{MUT} = G'_{MUT} - G = \frac{1}{2Z_o}\left\{\frac{|S_{21}|_{\omega_{0,MUT}}}{1-|S_{21}|_{\omega_{0,MUT}}} - \frac{|S_{21}|_{\omega_{0,b}}}{1-|S_{21}|_{\omega_{0,b}}}\right\} \quad (10)$$

The loss tangent of the MUT is given by

$$\tan\delta_{MUT} = \frac{G_{MUT}}{(C'_{MUT} - C_{subs})\omega_{0,MUT}} \quad (11)$$

where C_{subs} is the substrate contribution to the capacitance of the DB-DGS resonator (and, consequently, $C'_{MUT} - C_{subs}$ is the contribution of the MUT to the capacitance of the DB-DGS). C_{subs} is given by [10]

$$C_{subs} = C\frac{\varepsilon_r}{\varepsilon_{r,eq} + 1} \quad (12)$$

Introducing (12) and (3) in (11), the following expression is obtained

$$\tan\delta_{MUT} = \frac{G_{MUT}(\varepsilon_{r,eq} + 1)}{C\,\varepsilon_{MUT}\,\omega_{0,MUT}} \quad (13)$$

Finally, introducing (10) in (13), the loss tangent is found to be

$$\tan\delta_{MUT} = \frac{\varepsilon_{r,eq} + 1}{2Z_o C\,\varepsilon_{MUT}\,\omega_{0,MUT}}\left\{\frac{|S_{21}|_{\omega_{0,MUT}}}{1-|S_{21}|_{\omega_{0,MUT}}} - \frac{|S_{21}|_{\omega_{0,b}}}{1-|S_{21}|_{\omega_{0,b}}}\right\} \quad (14)$$

and it can be inferred from the measured responses of the bare sensor and sensor loaded with the MUT (provided all the parameters preceding the brackets in (14) are either known or previously inferred, e.g., ε_{MUT}).

At this point, it should be mentioned that the capacitance appearing in the denominator in (11), i.e., the contribution of the MUT to the capacitance of the DB-DGS, $C'_{MUT} - C_{subs}$, is not C_{MUT}. The latter is simply the difference between the total capacitance of the loaded DB-DGS, C'_{MUT} and the capacitance of the unloaded DB-DGS, C, which includes the contribution of air, C_{air}. In other words, $C_{MUT} = C'_{MUT} - C \neq C'_{MUT} - C_{subs}$, since $C = C_{subs} + C_{air}$. By contrast, the whole conductance of the loaded DB-DGS is $G'_{MUT} = G + G_{MUT}$, as indicated before, where G is the conductance of the bare DB-DGS, which coincides with the conductance of the substrate ($G = G_{subs}$), provided the conductance of air is null, and G_{MUT} is the contribution to the conductance of the MUT. Figure 5 shows the different contributions to the capacitance and conductance of the bare and loaded DB-DGS.

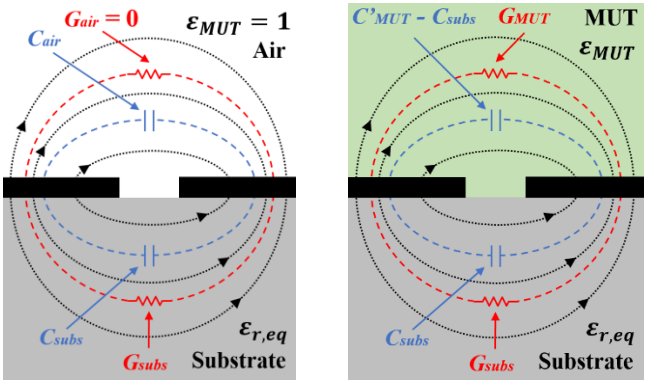

(a) (b)

Fig. 5. Sketch showing the different contributions to the capacitance and conductance of the bare (a) and loaded (b) DB-DGS resonator.

V. Validation

To validate the previous analysis, different MUT samples with well-known electromagnetic parameters (dielectric constant and loss tangent) have been considered. In particular, we have used three solid samples and DI water. The solid samples are uncladded microwave substrates (*Rogers RO4003C* and *RO3010*) and FR4. Actually, three 1.5-mm thick slabs have been stacked (and glued) in order to achieve the necessary MUT thickness to guarantee the validity of the semi-infinite MUT approximation. Concerning DI water, a container was fabricated by means of a 3D printer (model *Ultimaker 3 Extended*) using Polylactic-Acid (PLA) material, and then it was attached to the substrate, on top of the DB-DGS resonator. Such container is high enough to ensure that the height of the liquid (DI water) suffices to consider it semi-infinite in the vertical direction, as required. For the measurement with DI water, the substrate was protected with a dry film of clear polyester (with an estimated dielectric constant of 3.5 and thickness of 50-μm), in order to avoid substrate absorption. The effects of such thin film are negligible given the high dielectric constant of DI water. Figure 6 depicts the photograph of the bare sensor (sensor A) and the sensor equipped with the liquid container. The sensor was fabricated with the *LPKF H100* drilling machine.

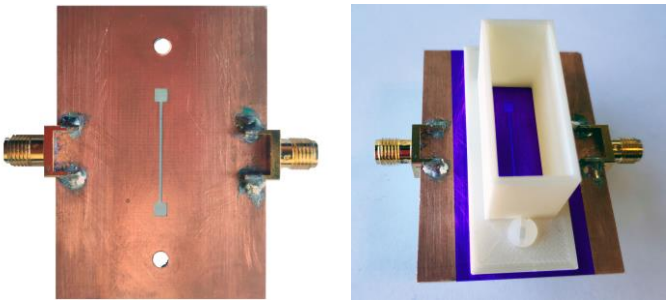

(a) (b)

Fig. 6. Photograph of the fabricated sensor (a), and sensor including the liquid container (b).

The simulated (using *ANSYS HFSS*) and measured (by means of the *Keysight N5221A* vector network analyzer) frequency

responses of the bare sensor, and sensor loaded with the different MUT samples, are depicted in Fig. 7, where good agreement is obtained in all the cases. Nevertheless, note that in FR4, the non-negligible (but acceptable) frequency shift between measurement and simulation is attributed to the well-known tolerances (uncertainties) in the dielectric constant of such material. The nominal dielectric constant and loss tangent for the considered MUTs are indicated in Table II. Application of expression (6) to the simulated and measured responses, with $f_{0,b}$ and $f_{0,MUT}$ easily identifiable from the results, provides the MUT dielectric constants also indicated in the table and identified as simulated (sim.) and experimental (exp.). Similarly, using (14), with the notch depths inferred from the simulated and the measured responses, the loss tangents of the MUTs are obtained (the results are also included in Table II).

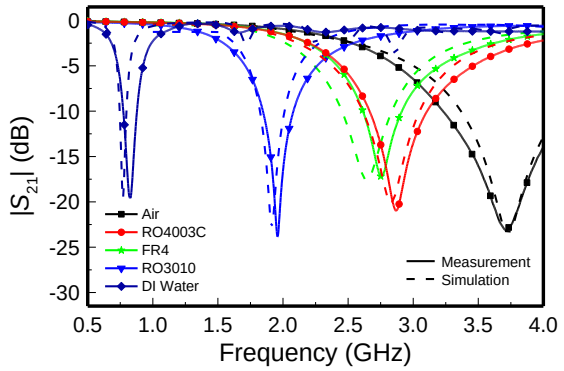

Fig. 7. Measured responses (transmission coefficient) of the bare sensor and sensor loaded with stacks of *FR4*, *Rogers RO3010*, and *Rogers RO4003C*, as well as DI water.

TABLE II
MUT PARAMETERS

	RO4003C	FR4	RO3010	DI Water
ε_{MUT} (nom.)	3.55	4.40	10.2	80.9
tanδ (nom.)	0.0022	0.020	0.0020	0.042
ε_{MUT} (sim.)	3.57	4.44	10.6	79.5
tanδ (sim.)	0.0030	0.035	0.0022	0.050
ε_{MUT} (exp.)	3.53	4.05	10.0	78.2
tanδ (exp.)	0.0017	0.039	0.0022	0.041

As it can be appreciated from Table II, the reported analytical procedure provides the material parameters of the different MUTs to a good approximation, particularly the dielectric constant. The dielectric constant of FR4 inferred from the measured notch frequency is moderately smaller than the nominal value. This is an expected result taking into account the frequency deviation visible in Fig. 7, and attributed to the high dispersion of this parameter from sample to sample in FR4. The loss tangent of the MUT cannot be accurately predicted, in part because expression (14) is highly sensitive to variations in the notch depth, which can be caused by diverse factors (e.g., air gaps between stacked layers, and with the substrate, effects of connectors, etc.). Nevertheless, the proposed sensor, using the reported analytical procedure, is able to provide a rough estimation of the loss tangent of the MUT (or order of magnitude). It is well known that the accurate measurement of the loss tangent in low-loss solid samples requires methods based on resonant cavities [45], bulky and expensive as compared to the proposed method. Nevertheless, let us mention that, in order to minimize the well-known effects of the air gap, we have pressed the MUT samples against the substrate by means of screws.

VI. COMPARISON TO OTHER APPROACHES

A meaningful comparison between microwave permittivity sensors based on frequency variation and reported in the literature is not simple. In particular, comparing the relative sensitivity, the main figure of merit in these sensors, is not absent of certain difficulty, since this parameter is not constant (it depends on the dielectric constant of the MUT), and it varies (decreases) with the substrate dielectric constant. In many comparison tables reported in the literature, the relative average sensitivity is the considered parameter subject of comparison. However, since the relative sensitivity decreases with the dielectric constant of the MUT, it follows that the relative average sensitivity depends significantly on the considered input dynamic range of the dielectric constant of the MUT. Thus, a significant comparison requires that the considered input dynamic ranges are similar. According to these comments, and because one of the considered MUTs in this work is DI water, with measured dielectric constant of 78.2 (see Table II), we have compared the sensor proposed in this work with other sensors exhibiting an input dynamic range (in the dielectric constant) of the same order. Table III reports such comparison. In the table, $f_{0,b}$ is the frequency of the bare resonator. S_{av} is the average sensitivity, calculated as the ratio between the output dynamic range (or difference between the resonance frequency of the bare resonator and the resonance frequency of the resonator loaded with the MUT exhibiting the maximum dielectric constant) and the input dynamic range (difference between the maximum and minimum values of ε_{MUT}). Finally, $\bar{S}_{av}$ is the relative average sensitivity, calculated by simply dividing the average sensitivity by the resonance frequency of the bare resonator, i.e., $\bar{S}_{av} = S_{av}/f_{0,b}$ (nevertheless, note that in the table, $\bar{S}_{av}$ is expressed as percentage). The table includes also the considered input dynamic range relative to the dielectric constant of the MUT.

TABLE III
COMPARISON OF VARIOUS SENSORS IN TERMS OF SENSITIVITY

Reference	$f_{0,b}$ (GHz)	S_{av} (MHz)	$\bar{S}_{av}$ (%)	Din. Range
[2]	1.9	1.53	0.081	9.0-80.0
[4]	2.0	4.76	0.238	9.0-79.5
[6]	3.5	9.16	0.261	6.5-80.0
[8]	0.87	0.79	0.091	27.8-80.8
This work	3.75	38.21	1.019	1.0-78.2

According to the results of Table III, the proposed sensor exhibits by far the higher relative average sensitivity. It should be mentioned that the substrate dielectric constant in the sensors of [2],[8] is ε_r = 10.2, and this explains in part the limited relative average sensitivity in such sensors. However, in the sensors reported in [4] and [6], the dielectric constant of the substrate is ε_r = 2.94 and ε_r = 2.33, respectively, i.e., smaller

than the one considered in the sensor proposed in this work (ε_r = 3.55). The reason that explains the superior relative average sensitivity in the present work is the considered resonator, a DB-DGS. With this sensing resonant element, the changes in the dielectric constant of the MUT directly affect the unique capacitance that determines the resonance frequency, the output variable. By contrast, in the sensors presented in [4],[6], where a complementary split ring resonator (CSRR) was used, the resonance frequency is also dependent on the coupling capacitance between the line and the resonant element. Since such capacitance does not vary with the dielectric constant of the MUT, it is expected that such CSRR-based sensors exhibit poorer sensitivity, as compared to those of DB-DGS-based sensors, as it actually occurs. In other words, the coupling capacitance of the CSRR obscures in part the effects of the dielectric constant of the MUT on the variation of the resonance frequency, thereby reducing the sensitivity.

There are other recently reported sensors based on frequency variation that exhibit good performance, especially high sensitivity [46],[47]. However, such sensors have been applied to MUT samples exhibiting much smaller input dynamic range, and for this main reason, they are not included in the comparative Table III.

Concerning the measurement of the loss tangent in low-loss solid samples by means of planar sensors, papers [19],[20] present sensing structures based on CSRRs in both cases. Such sensors provide not only the dielectric constant of the MUT, but also the loss tangent, similar to the sensor reported in this work. However, the accuracy in the determination of the loss tangent with those sensors is comparable to that of the sensor of Fig. 6, i.e., it is limited (an inherent characteristic of planar sensors). Consequently, the loss factor of the MUT can be roughly estimated with these (planar) sensors, rather than being accurately predicted.

To end this section, let us mention that for the measurement of complex variables, or for the characterization of complex phenomena, such as corrosion, among others, post processing algorithms such as feature fusion, as discussed in the [48], involving multi-frequency measurements, are useful in order to improve the sensitivity and reliability of the sensor. There are also statistical methods useful for estimation of multiple parameters, such as the so-called principal component analysis (PCA) [49]. The sensor reported in this paper is devoted to dielectric constant measurements, and therefore such methods have not been applied. Let us also mention that there are different variables intimately related to the complex dielectric constant. Thus, such variables can potentially be retrieved with the proposed sensor. Nevertheless, for multivariable measurements or, for example, for the determination of material composition in complex samples, multi-frequency measurements are also needed (see e.g. [50]). Application of such type of measurements with DB-DGS resonators is left for a future work.

VII. Conclusions

In summary, an analytical method to determine the dielectric constant and loss tangent of solids and liquids in DB-DGS-based frequency-variation permittivity sensors has been reported and experimentally validated. The method is based on analytical expressions that depend on the notch frequency and magnitude of the response of the bare sensor and sensor loaded with the MUT, i.e., easily measurable quantities. The results obtained by considering samples with known dielectric constant and loss tangent (including low-loss microwave substrates, FR4 and DI water) have demonstrated the accuracy of the method for the determination of the dielectric constant. The loss tangent, related to the notch magnitude, cannot be estimated with the same level of accuracy, but the method has been demonstrated to provide a rough estimate of the nominal value. Moreover, a sensitivity analysis, that demonstrates that the relative sensitivity (the main figure of merit in frequency variation sensors) does not depend on the geometry of the DB-DGS resonator (for thick enough substrates), has been carried out in the paper. It has been found that the sensitivity can be optimized by decreasing the dielectric constant of the substrate, and it decreases with the dielectric constant of the MUT. The proposed DB-DGS frequency-variation permittivity sensor exhibits higher relative sensitivity as compared to other sensors based on slot resonators, such as CSRR-based permittivity sensors. Since microstrip lines with slot resonators etched in the ground plane are very interesting permittivity sensors, due to the inherent backside isolation of the ground plane, it can be concluded that DB-DGS-loaded microstrip lines are very promising devices for permittivity sensing. Such devices not only exhibit superior sensitivity than their CSRR-based counterparts, but also, a simple circuit model describes them, and the sensors can be easily designed with the optimum (relative) sensitivity, since it mainly depends on the substrate dielectric constant.

References

[1] K. Grenier et al., “Integrated broadband microwave and microfluidic sensor dedicated to bioengineering,” *IEEE Trans. Microw. Theory Techn.*, vol. 57, no. 12, pp. 3246–3253, Dec. 2009.

[2] W. Withayachumnankul, K. Jaruwongrungsee, A. Tuantranont, C. Fumeaux, and D. Abbott, “Metamaterial-based microfluidic sensor for dielectric characterization,” *Sens. Actuators A, Phys.*, vol. 189, pp. 233-237, Jan. 2013.

[3] T. Chretiennot, D. Dubuc, and K. Grenier, “A microwave and microfluidic planar resonator for efficient and accurate complex permittivity characterization of aqueous solution”, *IEEE Trans. Microw. Theory Techn.*, vol. 61, no. 2, pp. 972-978, Feb. 2013.

[4] A. Ebrahimi, W. Withayachumnankul, S. Al-Sarawi, D. Abbott, “High-sensitivity metamaterial-inspired sensor for microfluidic dielectric characterization,” *IEEE Sensors J.*, vol. 14, no. 5, pp. 1345−1351, May 2014.

[5] A. Ebrahimi, W. Withayachumnankul, S.F. Al-Sarawi, and D. Abbott, “Microwave microfluidic sensor for determination of glucose concentration in water,” in *2015 IEEE 15th Mediterranean Microwave Symposiu*m (MMS), 2015, pp. 1–3.

[6] A. Salim and S. Lim, “Complementary split-ring resonator-loaded microfluidic ethanol chemical sensor,” *Sensors*, vol. 16, pp. 1–13, 2016.

[7] M. H. Zarifi and M. Daneshmand, “Liquid sensing in aquatic environment using high quality planar microwave resonator,” *Sens. Actuators B, Chem.*, vol. 225, pp. 517–521, Mar. 2016.

[8] P. Vélez, L. Su, K. Grenier, J. Mata-Contreras, D. Dubuc, and F. Martín, "Microwave microfluidic sensor based on a microstrip splitter/combiner configuration and split ring resonators (SRR) for dielectric

characterization of liquids", *IEEE Sensors J.*, vol. 17, pp. 6589-6598, Aug. 2017.

[9] P. Vélez, K. Grenier, J. Mata-Contreras, D. Dubuc, and F. Martín, "Highly-sensitive microwave sensors based on open complementary split ring resonators (OCSRRs) for dielectric characterization and solute concentration measurement in liquids", *IEEE Access*, vol. 6, pp, 48324-48338, 2018.

[10] L. Su, J. Mata-Contreras, P. Vélez, A. Fernández-Prieto, and F. Martín, "Analytical method to estimate the complex permittivity of oil samples", *Sensors*, vol. 18, p. 984, 2018.

[11] M. Abdolrazzaghi, M. Daneshmand, A. K. Iyer, "Strongly enhanced sensitivity in planar microwave sensors based on metamaterial coupling", *IEEE Trans. Microw. Theory Techn*., vol. 66, no. 4, pp. 1843-1855, Jan. 2018.

[12] M.H. Zarifi, H. Sadabadi, S.H. Hejazi, M. Daneshmand, A. Sanati-Nezhad, "Noncontact and nonintrusive microwave-microfluidic flow sensor for energy and biomedical engineering", *Sci. Rep*., vol. 8 (1), pp. 139, 2018.

[13] P. Vélez, J. Muñoz-Enano, K. Grenier, J. Mata-Contreras, D. Dubuc, F. Martín, "Split ring resonator (SRR) based microwave fluidic sensor for electrolyte concentration measurements", *IEEE Sensors J*., vol. 19, pp. 2562-2569, Apr. 2019.

[14] J. Muñoz-Enano, P. Vélez, J. Mata-Contreras, M. Gil, D. Dubuc, K. Grenier, F. Martín, "Microwave sensors/comparators with optimized sensitivity based on microstrip lines loaded with open split ring resonators (OSRRs)", *49th European Microwave Conference*, Paris, France, Sep.-Oct. 2019.

[15] P. Vélez, J. Muñoz-Enano, F. Martín, "Electrolyte concentration measurements in DI water with 0.125g/L resolution by means of CSRR-based structures", *49th European Microwave Conference*, Paris, France, Sep.-Oct. 2019.

[16] M. Puentes, Planar Metamaterial Based Microwave Sensor Arrays for Biomedical Analysis and Treatment, Springer, Heidelberg, Germany, 2014.

[17] M. Schueler, C. Mandel, M. Puentes, and R. Jakoby, "Metamaterial inspired microwave sensors," *IEEE Microw. Mag.*, vol. 13, no. 2, pp. 57–68, Mar. 2012.

[18] M. S. Boybay and O. M. Ramahi, "Material characterization using complementary split-ring resonators," *IEEE Trans. Instrum. Meas*., vol. 61, no. 11, pp. 3039−3046, Nov. 2012.

[19] C.-S. Lee and C.-L. Yang, "Complementary split-ring resonators for measuring dielectric constants and loss tangents," *IEEE Microw. Wireless Compon. Lett.*, vol. 24, pp. 563-565, Aug. 2014.

[20] C.-L. Yang, C.-S. Lee, K.-W. Chen, and K.-Z. Chen, "Noncontact measurement of complex permittivity and thickness by using planar resonators," *IEEE Trans. Microw. Theory Techn.*, vol. 64, pp. 247−257, Jan. 2016.

[21] A. K. Horestani, J. Naqui, Z. Shaterian, D. Abbott, C. Fumeaux, and F. Martín, "Two-dimensional alignment and displacement sensor based on movable broadside-coupled split ring resonators," Sens. Actuators A, vol. 210, pp. 18–24, Apr. 2014.

[22] L. Su, J. Naqui, J. Mata-Contreras, and F. Martín "Modeling metamaterial transmission lines loaded with pairs of coupled split ring resonators," IEEE Ant. Wireless Propag. Lett., vol. 14, pp. 68–71, 2015.

[23] L. Su, J. Naqui, J. Mata-Contreras, and F. Martín, "Modeling and applications of metamaterial transmission lines loaded with pairs of coupled complementary split ring resonators (CSRRs)," *IEEE Ant. Wireless Propag. Lett*., vol. 15, pp. 154–157, 2016.

[24] J. Naqui, C. Damm, A. Wiens, R. Jakoby, L. Su, J. Mata-Contreras, and F. Martín, "Transmission lines loaded with pairs of stepped impedance resonators: modeling and application to differential permittivity measurements", *IEEE Trans. Microw. Theory Techn*., vol. 64, no. 11, pp. 3864-3877, Nov. 2016.

[25] L. Su, J. Mata-Contreras, J. Naqui, and F. Martín, "Splitter/combiner microstrip sections loaded with pairs of complementary split ring resonators (CSRRs): modeling and optimization for differential sensing applications," IEEE Trans. Microw. Theory Techn., vol. 64, pp. 4362-4370, Dec. 2016.

[26] J. Naqui, M. Durán-Sindreu and F. Martín, "Novel sensors based on the symmetry properties of split ring resonators (SRRs)," Sensors, vol 11, pp. 7545−7553, 2011.

[27] J. Naqui, M. Durán-Sindreu, and F. Martín, "Transmission Lines Loaded with Bisymmetric Resonators and Applications", IEEE MTT-S Int. Microw. Symp., June 2013, Seatle (USA).

[28] J. Naqui, M. Durán-Sindreu, and F. Martín, "Alignment and position sensors based on split ring resonators," Sensors, vol. 12, pp. 11790−11797, 2012.

[29] A.K. Horestani, C. Fumeaux, S.F. Al-Sarawi, and D. Abbott, "Displacement sensor based on diamond-shaped tapered split ring resonator," IEEE Sens. J., vol. 13, pp. 1153–1160, 2013.

[30] A.K. Horestani, D. Abbott, C. Fumeaux, "Rotation sensor based on horn-shaped split ring resonator," IEEE Sens. J., vol. 13, pp. 3014–3015, 2013.

[31] J. Naqui and F. Martín, "Transmission lines loaded with bisymmetric resonators and their application to angular displacement and velocity sensors," IEEE Trans. Microw. Theory Techn., vol. 61, no. 12, pp. 4700–4713, Dec. 2013.

[32] J. Naqui and F. Martín, "Angular displacement and velocity sensors based on electric-LC (ELC) loaded microstrip lines," IEEE Sensors J., vol. 14, no. 4, pp. 939–940, Apr. 2014.

[33] A.K. Horestani, J. Naqui, D. Abbott, C. Fumeaux, and F. Martín, "Two-dimensional displacement and alignment sensor based on reflection coefficients of open microstrip lines loaded with split ring resonators," Elec. Lett., vol. 50, pp. 620–622, Apr. 2014.

[34] J. Naqui and F. Martín, "Microwave sensors based on symmetry properties of resonator-loaded transmission lines: a review," Journal Sens., vol. 2015, Article ID 741853, 10 pages, 2015.

[35] J. Naqui, J. Coromina, A. Karami-Horestani, C. Fumeaux, and F. Martín, "Angular displacement and velocity sensors based on coplanar waveguides (CPWs) loaded with S-shaped split ring resonator (S-SRR)," Sensors, vol. 15, pp. 9628–9650, 2015.

[36] A. Ebrahimi, J. Scott, K. Ghorbani, "Differential sensors using microstrip lines loaded with two split-ring resonators", *IEEE Sensors J.*, vol. 18 (14), pp. 5786-5793, 2018.

[37] J. Naqui, *Symmetry Properties in Transmission Lines Loaded with Electrically Small Resonators: Circuit Modeling and Applications*, Springer, Heidelberg, Germany, 2016.

[38] J. Muñoz-Enano, P. Vélez, L. Su, M. Gil, P. Casacuberta and F. Martín, "On the Sensitivity of Reflective-Mode Phase-Variation Sensors Based on Open-Ended Stepped-Impedance Transmission Lines: Theoretical Analysis and Experimental Validation," *IEEE Trans. Microw. Theory Techn*., vol. 69, no. 1, pp. 308-324, Jan. 2021.

[39] L. Su, J Muñoz-Enano, P. Vélez, M. Gil, P. Casacuberta, and F. Martín, "Highly sensitive reflective-mode phase-variation permittivity sensor based on a coplanar waveguide (CPW) terminated with an open complementary split ring resonator (OCSRR)", *IEEE Access*, vol. 9, pp. 27928-27944, 2021.

[40] A. Ebrahimi, J. Scott, and K. Ghorbani, "Ultrahigh-Sensitivity Microwave Sensor for Microfluidic Complex Permittivity Measurement", *IEEE Trans. Microw. Theory Tech*., vol. 67, pp 4269-4277, 2019.

[41] D. Ahn, J. S. Park, C. S. Kim, Y. Qian, and T. Itoh "A Design of the lowpass filter using the novel microstrip defected ground structure," *IEEE Trans. Microw. Theory Techn*., vol. 49, no.1, pp. 86-93, Jan. 2001.

[42] P. Vélez, J. Muñoz-Enano, M. Gil, J. Mata-Contreras, and F. Martín, "Differential Microfluidic Sensors Based on Dumbbell-Shaped Defect Ground Structures in Microstrip Technology: Analysis, Optimization, and Applications" , *Sensors*, vol. 19, no. 14, paper 3189, 2019.

[43] L. Su, P. Vélez, J. Muñoz-Enano, and F. Martín, "Discussion and Analysis of Dumbbell Defect-Ground-Structure (DB-DGS) Resonators for Sensing Applications from a Circuit Theory Perspective," *Sensors*, vol. 21, no. 24, paper 8334, 2021.

[44] J. Muñoz-Enano, J. Martel, P. Vélez, F. Medina, L. Su, and F. Martín, "Parametric analysis of the edge capacitance of uniform slots and application to frequency-variation permittivity sensors", *Appl. Sci.*, vol. 11, paper 7000, 2021.

[45] M. D. Janezic, E. F. Kuester, and J. Baker-Jarvis, "Broadband complex permittivity measurements of dielectric substrates using a split-cylinder resonator," *IEEE MTT-S Int. Microw. Symp. Digest*, Fort Worth, TX, USA, Jun. 2004, pp. 1817-1820.

[46] A. Ebrahimi, J. Scott and K. Ghorbani, "Transmission Lines Terminated With LC Resonators for Differential Permittivity Sensing," *IEEE Microw. Wireless Compon. Lett.*, vol. 28, no. 12, pp. 1149-1151, Dec. 2018.

[47] A. Ebrahimi, Amir, G. Beziuk, J. Scott, and K. Ghorbani, "Microwave Differential Frequency Splitting Sensor Using Magnetic-LC Resonators," *Sensors*, vol. 20, no. 4, paper 1066, 2020.

[48] A. M. J. Marindra and G. Y. Tian, "Chipless RFID sensor for corrosion characterization based on frequency selective surface and feature fusion," *Smart Mater. Struct*., vol. 29 paper 125010, 2020.

[49] A. M. J. Marindra and G. Y. Tian, "Multiresonance Chipless RFID Sensor Tag for Metal Defect Characterization Using Principal Component Analysis," *IEEE Sensors J.*, vol. 19, no. 18, pp. 8037-8046, Sep. 2019.

[50] N. Hosseini and M. Baghelani, "Selective real-time non-contact multi-variable water-alcohol-sugar concentration analysis during fermentation process using microwave split-ring resonator based sensor," *Sens. Act. A: Phys*., vol. 325, pp, 112695, 2021.

Jonathan Muñoz-Enano was born in Mollet del Vallès (Barcelona) Barcelona, Spain, in 1994. He received the Bachelor's Degree in Electronic Telecommunications Engineering in 2016 and the Master's Degree in Telecommunications Engineering in 2018, both at the Autonomous University of Barcelona (UAB). Actually, he is working in the same university in the elaboration of his PhD, which is focused on the development of microwave sensors based on metamaterials concepts for the dielectric characterization of materials and biosensors.

Paris Vélez (S'10–M'14–SM'21) was born in Barcelona, Spain, in 1982. He received the degree in Telecommunications Engineering, specializing in electronics, the Electronics Engineering degree, and the Ph.D. degree in Electrical Engineering from the Universitat Autònoma de Barcelona, Barcelona, in 2008, 2010, and 2014, respectively. His Ph.D. thesis concerned common mode suppression differential microwave circuits based on metamaterial concepts and semi-lumped resonators. During the Ph.D., he was awarded with a pre-doctoral teaching and research fellowship by the Spanish Government from 2011 to 2014. From 2015-2017, he was involved in the subjects related to metamaterials sensors for fluidics detection and characterization at LAAS-CNRS through a TECNIOSpring fellowship cofounded by the Marie Curie program. From 2018 to 2021 he has worked in miniaturization of passive circuits RF/microwave and sensors-based metamaterials through Juan de la Cierva fellowship. His current research interests include the miniaturization of passive circuits RF/microwave and sensors-based metamaterials. Dr. Vélez is a Reviewer for the IEEE TRANSACTIONS ON MICROWAVE THEORY AND TECHNIQUES and for other journals.

Marta Gil (S'05-M'09) was born in Valdepeñas, Ciudad Real, Spain, in 1981. She received the Physics degree from Universidad de Granada, Spain, in 2005, and the Ph.D. degree in electronic engineering from the Universitat Autònoma de Barcelona, Barcelona, Spain, in 2009. She studied one year with the Friedrich Schiller Universität Jena, Jena, Germany. During her PhD Thesis she was holder of a METAMORPHOSE NoE grant and National Research Fellowship from the FPU Program of the Education and Science Spanish Ministry. As a postdoctoral researcher, she was awarded with a Juan de la Cierva fellowship working in the Universidad de Castilla-La Mancha. She was postdoctoral researcher in the Institut für Mikrowellentechnik und Photonik in Technische Universität Darmstadt and in the Carlos III University of Madrid. She is currently associate professor in the Universidad Politécnica de Madrid within the Excellence Program for University Professoriat of the V Regional Plan for Scientific Research and Technological Innovation of the Administration of the Community of Madrid. She has worked in metamaterials, piezoelectric MEMS and microwave passive devices. Her current interests include metamaterials sensors for fluidic detection.

Ferran Martín (M'04-SM'08-F'12) was born in Barakaldo (Vizcaya), Spain in 1965. He received the B.S. Degree in Physics from the Universitat Autònoma de Barcelona (UAB) in 1988 and the PhD degree in 1992. From 1994 up to 2006 he was Associate Professor in Electronics at the Departament d'Enginyeria Electrònica (Universitat Autònoma de Barcelona), and since 2007 he is Full Professor of Electronics. In recent years, he has been involved in different research activities including modelling and simulation of electron devices for high frequency applications, millimeter wave and THz generation systems, and the application of electromagnetic bandgaps to microwave and millimeter wave circuits. He is now very active in the field of metamaterials and their application to the miniaturization and optimization of microwave circuits and antennas. Other topics of interest include microwave sensors and RFID systems, with special emphasis on the development of high data capacity chipless-RFID tags. He is the head of the Microwave Engineering, Metamaterials and Antennas Group (GEMMA Group) at UAB, and director of CIMITEC, a research Center on Metamaterials supported by TECNIO (Generalitat de Catalunya). He has organized several international events related to metamaterials and related topics, including Workshops at the IEEE International Microwave Symposium (years 2005 and 2007) and European Microwave Conference (2009, 2015 and 2017), and the Fifth International Congress on Advanced Electromagnetic Materials in Microwaves and Optics (Metamaterials 2011), where he acted as Chair of the Local Organizing Committee. He has acted as Guest Editor for six Special Issues on metamaterials and sensors in five International Journals. He has authored and co-authored over 650 technical conference, letter, journal papers and book chapters, he is co-author of the book on Metamaterials entitled Metamaterials with Negative Parameters: Theory, Design and Microwave Applications (John Wiley & Sons Inc.), author of the book Artificial Transmission Lines for RF and Microwave Applications (John Wiley & Sons Inc.), co-editor of the book Balanced Microwave Filters (Wiley/IEEE Press) and co-author of the book Time-Domain Signature Barcodes for Chipless-RFID and Sensing Applications (Springer). Ferran Martín has generated 21 PhDs, has filed several patents on metamaterials and has headed several Development Contracts.

Prof. Martín is a member of the IEEE Microwave Theory and Techniques Society (IEEE MTT-S). He is reviewer of the IEEE Transactions on Microwave Theory and Techniques and IEEE Microwave and Wireless Components Letters, among many other journals, and he serves as member of the Editorial Board of IET Microwaves, Antennas and Propagation, International Journal of RF and Microwave Computer-Aided Engineering, and Sensors. He is also a member of the Technical Committees of the European Microwave Conference (EuMC) and International Congress on Advanced Electromagnetic Materials in Microwaves and Optics (Metamaterials). Among his distinctions, Ferran Martín has received the 2006 Duran Farell Prize for Technological Research, he holds the Parc de Recerca UAB – Santander Technology Transfer Chair, and he has been the recipient of three ICREA ACADEMIA Awards (calls 2008, 2013 and 2018). He is Fellow of the IEEE and Fellow of the IET.